Journal of Hydrology 526 (2015) 221–230

Contents lists available at ScienceDirect

Journal of Hydrology

journal homepage: www.elsevier.com/locate/jhydrol

Drought prediction till 2100 under RCP 8.5 climate change scenarios for Korea

Chang-Kyun Park [a], Hi-Ryong Byun [a,*], Ravinesh Deo [b], Bo-Ra Lee [c]

[a] Department of Environmental Atmospheric Sciences, Pukyong National University, Yongsoro 45, Nam-Gu, Busan, Republic of Korea
[b] School of Agricultural, Computational and Environmental Sciences, International Centre for Climate Science, University of Southern Queensland, Springfield Campus, Australia
[c] Applied Meteorology Research Division, National Institute of Meteorological Research, Korea Meteorological Administration, Republic of Korea

ARTICLE INFO

Article history:
Available online 28 October 2014

Keywords:
EDI
Future drought
RCP 8.5
Global warming
Drought trend
Drought periodicity

SUMMARY

An important step in mitigating the negative impacts of drought requires effective methodologies for predicting the future events. This study utilises the daily Effective Drought Index (*EDI*) to precisely and quantitatively predict future drought occurrences in Korea over the period 2014–2100. The *EDI* is computed from precipitation data generated by the regional climate model (HadGEM3-RA) under the Representative Concentration Pathway (RCP 8.5) scenario. Using this data for 678 grid points (12.5 km interval) groups of cluster regions with similar climates, the G1 (Northwest), G2 (Middle), G3 (Northeast) and G4 (Southern) regions, are constructed. Drought forecasting period is categorised into the early phase (EP, 2014–2040), middle phase (MP, 2041–2070) and latter phase (LP, 2071–2100). Future drought events are quantified and ranked according to the duration and intensity. Moreover, the occurrences of drought (when, where, how severe) within the clustered regions are represented as a spatial map over Korea. Based on the grid-point averages, the most severe future drought throughout the 87-year period are expected to occur in Namwon around 2039–2041 with peak intensity (minimum *EDI*) −3.54 and projected duration of 580 days. The most severe drought by cluster analysis is expected to occur in the G3 region with a mean intensity of −2.85 in 2027. Within the spatial area of investigation, 6.6 years of drought periodicity and a slight decrease in the peak intensity is noted. Finally a spatial–temporal drought map is constructed for all clusters and time-periods under consideration.

1. Introduction

To be prepared for the detrimental consequences of drought, it is essential to predict their properties precisely and objectively using reliable and robust analytical techniques. Especially in Korea this importance is greater as droughts have been the greatest natural disaster in the history of the region (Byun and Han, 1994) with more extreme events already predicted in the near future (Byun et al., 2008). As global warming cascades into the next generation, a change in drought intensity and duration as considered by many studies is becoming a threat to humanity. Therefore any measures for mitigation and adaptation require careful assessment historical events and accurate representation of future drought based on new methodological approaches.

Based on voluminous accounts of scientific literature, global trend in drought events appears to be non-steady and significantly variable over spatial and temporal scales. A decreasing trend of drought was detected in the Garesou region in Iran (Golmohammadi et al., 2011), East Asia (Burke et al., 2006; Dai, 2013) and in most parts of China (Chen et al., 2013). By contrast, an increasing trend of the frequency and intensity has been pointed for the Thessaly region in Greece (Loukas et al., 2008), United Kingdom and France (Vidal et al., 2012; Vidal and Wade, 2009), East Asia (Manabe et al., 2004; Wang, 2005; Wetherald and Manabe, 2002), North America (Rind et al., 1990), Europe (Jones et al., 1996) and globally (Burke et al., 2006; Dai, 2013). For the case of Asia, not all drought classes but only the extreme events have been predicted to increase (Ke et al., 2012; Kim and Byun, 2009; Kim et al., 2010). In the case of Korea, only a few studies on drought forecasting have been conducted (Boo et al., 2004; Kwak et al., 2011; Lee and Kim, 2013; Kim et al., 2014). A primary finding out of these studies was the intensification of drought in the southern region although severe events were also expected to be reduced in the middle and Han River region (Lee and Kim, 2013).

Despite the large volume of literature on drought, contradictory results on future drought have been obtained, partly due to the inherent limitations in the various kinds of indices. Among the

* Corresponding author. Tel.: +82 51 629 6640; fax: +82 51 629 6638.
E-mail address: hrbyun@pknu.ac.kr (H.-R. Byun).

http://dx.doi.org/10.1016/j.jhydrol.2014.10.043
0022-1694/

more than 100 indices, the representative ones are the soil moisture (Wetherald and Manabe, 2002), Palmer Drought Severity Index (*PDSI*) (Palmer, 1965), Standardised Precipitation Index (*SPI*) (McKee et al., 1993) and Effective Drought Index (*EDI*) (Byun and Wilhite, 1999). The analysis of soil moisture shows increasing frequency of global dryness (Wetherald and Manabe, 2002; Manabe et al., 2004; Sheffield and Wood, 2008; Wang, 2005) whereas the *PDSI* shows intensification of drought (Jones et al., 1996; Rind et al., 1990) and an elongation of the spatial coverage (Burke et al., 2006; Dai, 2013). However, based on the *SPI*, trends of intensification of future drought (Loukas et al., 2008) and trends of decreasing frequency (Chen et al., 2013) have been noted. By contrast, the *EDI* found an increase in extreme drought events in spite of decreases in their overall cases (Ke et al., 2012; Kim and Byun, 2009; Kim et al., 2010). Clearly, the choice of the analytical metric appears to be a pertinent factor in future prediction of drought events (Taylor et al., 2012) (Burke, 2011; Burke and Brown, 2008).

Another limitation is the basic data of rainfall predictions based on widely disparate warming scenarios. For example, it is challenging to accurately project the trends of climate change based on the Special Report on Emissions Scenarios (SRES) (Nakićenović, 2000) or the imaginary greenhouse gas scenarios, which arbitrarily increased the CO_2 concentrations by factors of two to four. In the same hindsight, precipitation is perhaps the most challenging variable to predict. To empower a more realistic prediction of future climate, the 5th Assessment Report conducted by the Intergovernmental Panel for Climate Change (IPCC) introduced the Representative Concentration Pathway (RCP) (Moss et al., 2010). This scenario provides more rational basis for CO_2 concentrations compared to the previously used artificial emission schemes.

In addition to this, the spatial resolution of most Global Climate Models (GCMs) does not permit realistic representations of the climate of small landmasses. With the previous focuses of climate modelling experiments being generally on global rather than regional scales, and the relatively course grid intervals of GCMs, a significant constraint on spatially representative projection of precipitation is imposed. Consequently, the characteristics of future drought events, especially for small regions like Korea, which is a small part of Asia, are seldom considered realistically. It is therefore crucial that a re-evaluation of drought on the basis of new warming scenarios such as the RCP and regionally representative climate models is conducted for improving confidence in future predictions.

In order to realistically predict future drought, an appropriate drought index must be chosen. Although soil moisture-based index can deduce climatological conditions related to drought, the water-holding capacity for regions differs by the attributes of the soil. It is therefore, unreasonable to generalise results derived from soil moisture to explain potential drought conditions (Mitchell and Warrilow, 1987). Interestingly, the *PDSI* can be computed as a weekly metric (Rhee and Carbone, 2007; Trenberth et al., 2014) and therefore, identify the onset and characteristics of drought more clearly (Todd et al., 2013). However, the *PDSI* under-perform in mountainous regions or those with extreme variability in rainfall and run-off (Burke et al., 2006; Karl, 1986; Smith et al., 1993). The *SPI* operates over sliding timescales without objective regulations on the time-period and therefore hinders the detection dates of dry spells, short- and ongoing drought as stipulated by Kim et al. (2009). Both the *PDSI* and the *SPI* were originally designed for monthly timescales although conditions affected by drought can return to normal only with one day's rainfall (Byun and Wilhite, 1999). However, to date, many investigations including Morid et al. (2006), Kim et al. (2009) and Dogan et al. (2012) have found the *EDI* is a more ideal index for the diagnosis of dry spells, short and long-term drought events.

The purpose of this investigation is then fourfold: To determine the projections of drought in Korea predicted by precipitation data generated over regional scales using the daily *EDI*, to improve the predictability of future drought by employing realistic and skilful precipitation forecasts over Korea, to more precise quantification of drought that other drought indices, and to examine future projections of drought considering warming scenarios that assume that greenhouse gases will continue to elevate in parallel with the current trend with no reduction efforts.

2. Methodology

2.1. Climate model and precipitation data

Daily precipitation data generated by the regional climate model, HadGEM3-RA (Hewitt et al., 2011) for the period 2014–2100 was analysed. This model is based on the global atmospheric HadGEM3 of the Met Office Hadley Centre (MOHC). Rather than using the peak-and-decline scenario (RCP2.6) or stabilisation scenario (RCP6) where the total radiative forcing is stabilized shortly after 2100, we employ the RCP 8.5 scenarios that assumed the greenhouse gases continue to elevate according to the current trends (Riahi et al., 2011). Our goal is to project future drought based on the continuity of the present level of CO_2 emissions. Accordingly the CO_2 concentration is expected to rise to 1370 ppm by the year 2100 (Van Vuuren et al., 2011). In this study, the grid interval of the precipitation data extracted from the HadGEM3-RA model is 0.11° in latitude and longitude (12.5 km × 12.5 km). For analysis the time domain was divided into two periods, as the current (1971–2000) and the future (2014–2100) climate. The current period is based on rising trend of greenhouse gas concentration from the industrial revolution until the present day. For convenience sake, the future climate was sectioned into three 30-year segments, as the early (EP, 2014–2040), middle (MP, 2041–2070) and latter (LP, 2071–2100) phases.

Fig. 1 shows the spatial distribution of mean daily precipitation projected by the HadGEM3-RA and 61 weather station observational data from the Korean Meteorological Administration (KMA) for the period 1971–2000. Despite some differences between the observed and modelled datasets in the western parts of Korea, both plots depict high precipitation in the southern and northern parts of east coast, and low values in inland parts of Gyeongsang Province. Practically it is almost impossible to perfectly reproduce the natural precipitation trends by using a dynamic or physical model. It must thus be realised that the physical model output is rarely, if ever, directly compared with local climates without appropriate dynamical downscaling, as a mismatch of spatial scales between the projected and point-specific local climates is eminent (Palutikof et al., 1997). As dynamic models generally represent areal integrations over broad regions of interest (Portman et al., 1992; Skelly and Henderson-Sellers, 1996) one should be cautious of any direct comparison. Nevertheless, there are considerable advantages of broad comparison of observed and modelled data, as demonstrated in this work to establish a broader understanding of whether physical models can replicate overall observed conditions. In this work the HadGEM3-RA shows relatively good correspondence with modelled dataset. Therefore, the precipitation projections are considered appropriate for predicting future drought in Korea.

2.2. Computation of the Effective Drought Index

To predict future drought events, the Effective Drought Index (*EDI*) developed by Byun and Wilhite (1999) was employed for analysing daily precipitation derived the HadGEM3-RA model with

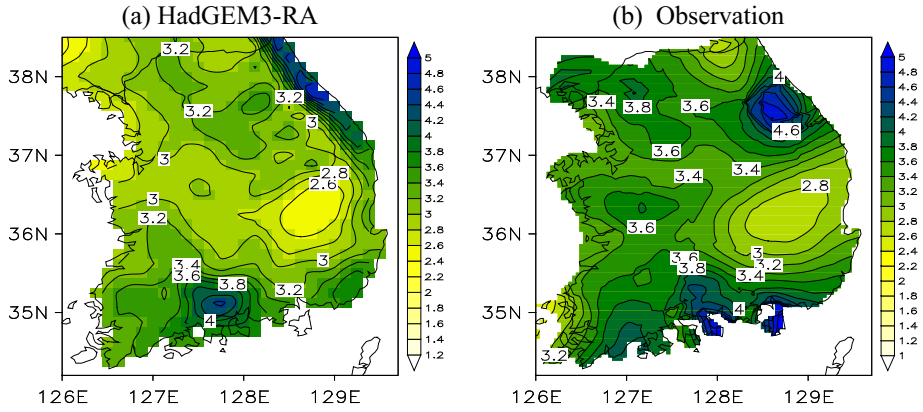

Fig. 1. Distribution of the 30-year (1971–2000) mean of daily precipitation over Korea from (a) 678 grid points of HadGEM3-RA model (projected dataset) and (b) 61 weather station data of KMA (observed dataset).

RCP 8.5 warming scenarios. The *EDI* was deduced from summed values of daily precipitation (*effective precipitation*) with time-dependent reduction functions to precisely detect any changes in drought on daily basis By utilising each day's effective precipitation relative to the climatological mean, this method has been proven to be a robust evaluative mechanism of drought events both over short and long-term scales (Kim et al., 2009; Morid et al., 2006; Kim and Byun, 2009; Dogan et al., 2012). A great advantage over the other kinds of indices is the ability of the daily *EDI* to detect the period of drought first, before the intensity or the duration of drought is calculated. The specific *EDI* equations are below.

$$ER = \sum_{n=1}^{i}\left[\left(\sum_{m=1}^{n} P_m\right)\Big/ n\right] \tag{1}$$

$$DER = ER - MER \tag{2}$$

$$EDI = DER/[ST(DER)] \tag{3}$$

where *ER* in Eq. (1) is effective precipitation with accumulated daily water resources based on previous day's precipitation considering the losses over time. P_m is the precipitation m days ago starting from the first day of the year and i is the duration of summation. It is fairly reasonable to use i as 365 days, which is a most dominant precipitation cycle worldwide. However, in the present study, one year was converted to 360 days by the model of the RCP 8.5 warming scenario, and the summating duration i followed it. Using the *DER* as the climatological (30-year) mean value of *ER* of the date, the *EDI* has been calculated as the standardised metric in Eq. (3). In general, a more negative *EDI* would indicate lower than normal daily water resources, thus signifying greater dryness value. For more details of this rather complex procedure, readers are referred to the original work of Byun and Wilhite (1999).

To analyse future drought using the current climate as the base period, the basic mathematical relations are modified slightly following Kim and Byun (2009).

$$DER_{CC} = ER_{CC} - MER_{CC} \tag{4}$$

$$EDI_{FC} = (ER_{FC} - MER_{CC})/ST(DER_{CC}) \tag{5}$$

Note that the subscripts *CC* and *FC* denote the current (1971–2000) and future climate (2014–2100), respectively. That is, ER_{CC} is the *ER* value of the current climate and ER_{FC} is the *ER* value of the future climate. Therefore, the *EDI* after the year 2014 has been designated as EDI_{FC}. Since the *EDI* is standardised metric whilst the *ER* values are normally distributed, the criterion for classifying drought intensity is different case by case. Table 1 explains the various intensity of dry levels as depicted by the *EDI*. In this study, the drought period was defined with the *EDI* being successively less than −0.5 when minimum *EDI* less than −1.0.

Table 1
Classification of dry level defined by the *EDI* in this study.

EDI	Dry level
$-0.5 \leqslant EDI \leqslant 0$	Normal
$-1.0 \leqslant EDI < -0.5$	Moderate
$-2.0 \leqslant EDI < -1.0$	Severe
$EDI < -2.0$	Extreme

2.3. Changes in projected precipitation

Fig. 2 displays the distribution of mean precipitation for the future periods EP, MP and LP, as well as the pairwise differences between the EP & CC, MP & EP, and LP & MP, respectively. It is clear that the data for MP generally exhibits higher precipitation than the other two counterparts except in most of the coastal regions in the period LP. This indicates that a monotonic trend in climate change is not eminent in the future. By contrast, it is surprising to note that over the coastal areas; continuously increasing precipitation throughout all periods are seen although the south coast exhibits a larger trend that is presumably driven by global warming.

In Fig. 3, the coefficient of variation (*CV*) of precipitation, which is deduced as the standard deviation divided by the mean, has been shown. Evidently, there is continuously increasing trend in the magnitude of *CV* for the western and central parts of Korea. Interestingly, some regions depict an increase in precipitation for the period LP (Fig. 2b), and supports more frequent flush style heavy rain in the long-term future.

2.4. Changes in future drought

2.4.1. Spatial distribution

Fig. 4 presents the drought cases for each period under consideration based on the characteristics in terms of the frequency per year, mean annual intensity and mean annual duration of drought. The highest frequency and duration of future drought is detected for the period EP, while and the highest intensity of drought is for MP. In southern parts of the west coast, the frequency of future is the lowest and the intensity is the highest for the period MP. This indicates that a severe drought event is expected to occur but may not be seriously elongated in terms of the duration of dry days.

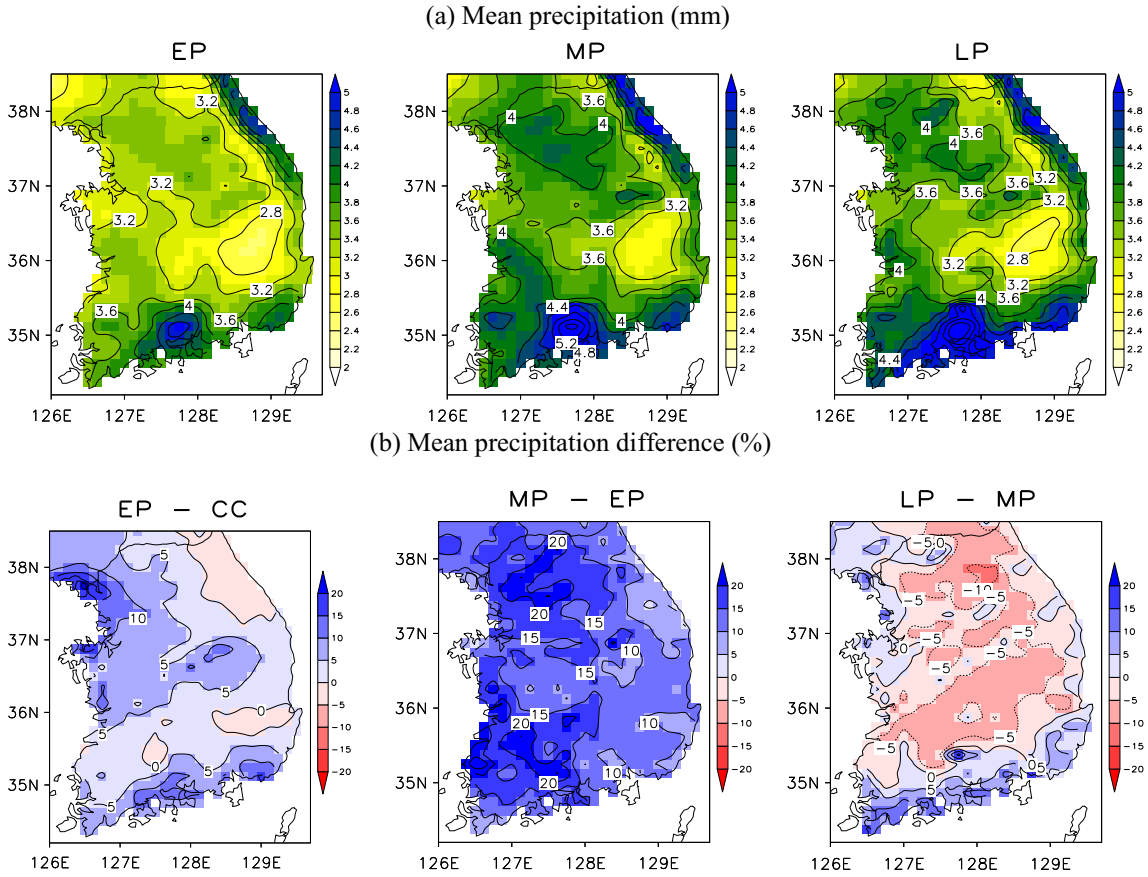

Fig. 2. Spatial distribution of (a) the 30-year mean of daily precipitation in each phase, (b) the percentages of the differences in 30-year mean precipitation, where the phases are current climate (CC, 1971–2000), early (EP, 2014–2040), middle (MP, 2041–2070) and latter (LP, 2071–2100).

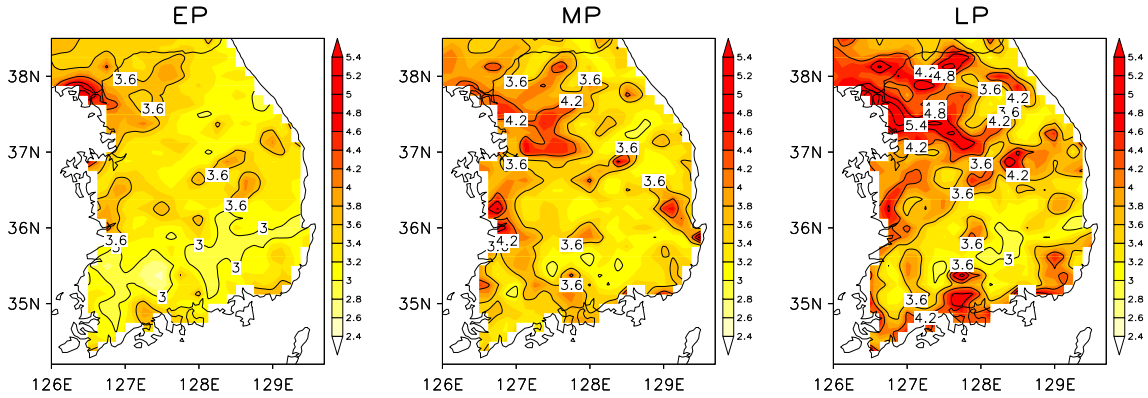

Fig. 3. Distribution of the coefficient of variation (*CV*) for the three future periods.

2.4.2. Drought ranking and spatial distributions

Next we assessed the severity and spatial distribution of future drought based on projected values of daily *EDI*. Tables 2 and 3 enumerates the properties of five high-ranked drought events based on drought intensity (minimum *EDI*) and drought duration (days with consecutively negative *EDI*). For events ranked by their intensity, there appears to be a reasonable positive correlation between the magnitudes of the two parameters of drought for all events except the projected one between 2032 and 2034. That is to say, the highest intensity future drought (minimum *EDI* −3.54) is projected to elongate for as long as 580 days and the lowest intensity future drought (minimum −2.97) only for 312 days (Table 2). This trend, however, is not apparent when the drought events are ranked by their actual duration parameter (Table 3). Interestingly, both the severe and intense drought and the long-term drought are projected to occur in the early phase (EP) period. Fig. 5 plots the geographic location of droughts. By a close observation, it can be seen that the most severe drought is predicted to occur between 2039 and 2041, near Namwon, Jeonnam Province. This event is expected to have an intensity of *EDI* = −3.54 and a dry duration of 580 days. Importantly, this event far exceeds the threshold of an extreme drought for which the *EDI* = −2.0. Notwithstanding this, this region is expected to experience the major drought from 2032 to 2033 too, which has also been ranked in the top five

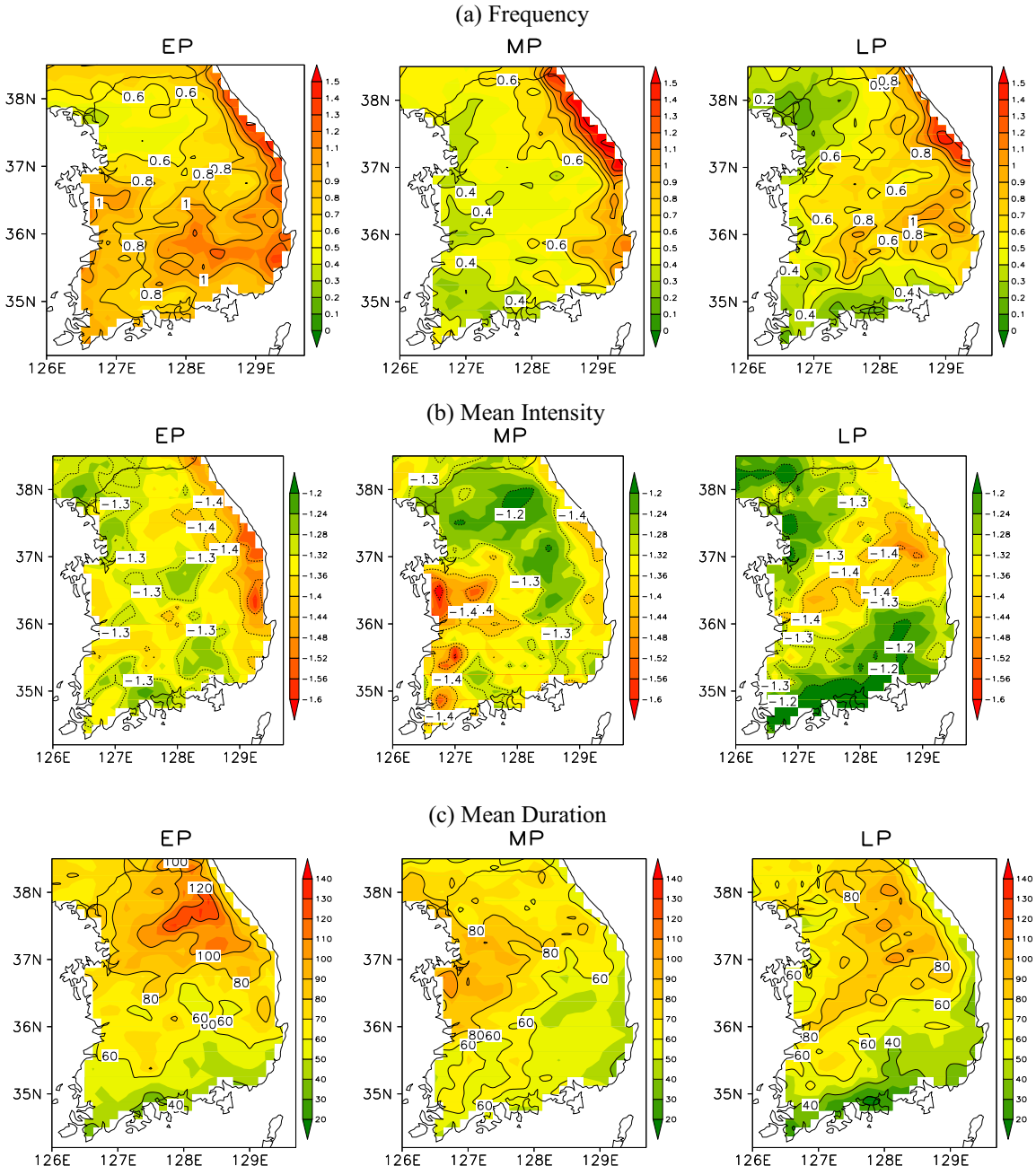

Fig. 4. Same as Fig. 2a except (a) frequency (per year), (b) intensity and (c) duration (days).

Table 2
The drought cases ranked by the intensity (minimum *EDI*).

Period	Ranking	Intensity	Start date	End date	Duration
All	1	−3.54	11 Sep 2039	21 Apr 2041	580
	2	−3.31	15 Jul 2026	30 Aug 2027	405
	3	−3.29	21 Mar 2040	13 Apr 2041	382
	4	−3.15	03 Jul 2032	10 Apr 2034	637
	5	−2.97	29 Jun 2032	11 May 2033	312

Table 3
The drought cases ranked by the duration (days).

Period	Ranking	Duration	Start date	End date	Intensity
All	1	716	23 Apr 2029	19 Apr 2031	−1.95
	2	683	15 Apr 2033	08 Mar 2035	−2.1
	3	640	28 May 2033	08 Mar 2035	−2.06
	4	637	03 Jul 2032	10 Apr 2034	−2.74
	5	580	11 Sep 2039	21 Apr 2041	−3.54

categories. The next severe case is expected to be realised in 2026–2027 in the northeast coast of Kangnung, Kangwon Province, with a peak intensity of −3.31.

Considering all projected drought cases in the present study, the longest duration spanning 716 days is expected to occur in Yang-gu, Kangwon Province, while 80% of the 10 severe droughts are projected to occur in the south-western parts (Fig. 5). It is noteworthy that based on these predictions, all of the severe and the longest droughts are expected to occur before 2041. This result agrees with findings of a previous study (Byun et al., 2008) which predicted an intense drought event to occur around the year 2025

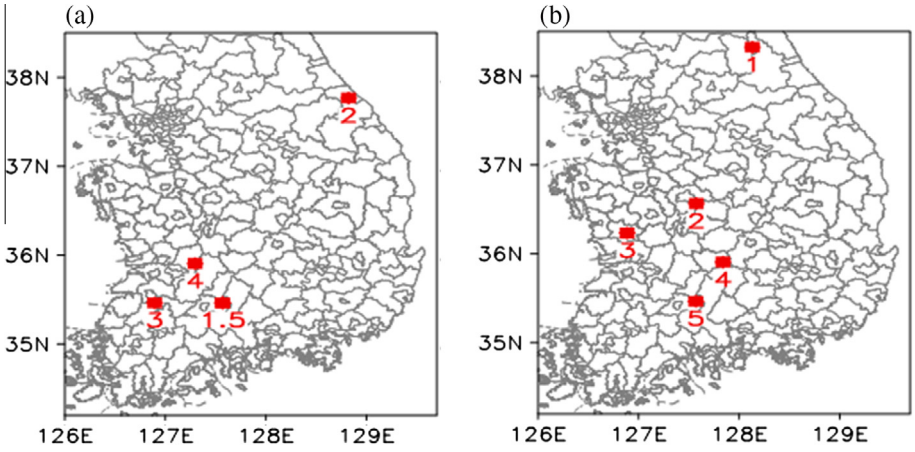

Fig. 5. The locations (red marks) of severe droughts in Tables 2(a) and 3(b). Grey lines depict the administrative section of Korea. (For interpretation of the references to color in this figure legend, the reader is referred to the web version of this article.)

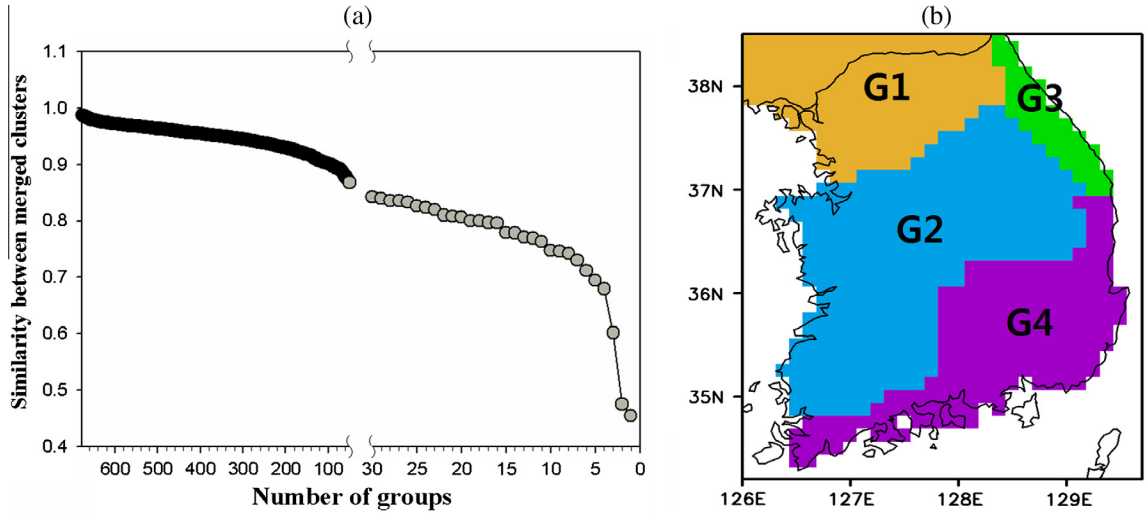

Fig. 6. (a) The variation of Pearson correlation coefficients between the two neighbours in group clusters. The numbers of groups vary from 677 to 1. (b) The distribution of 4 groups. G1 is Northwest region, G2 is Middle region, G3 is Northeast region, and G4 is Southern region.

using drought cycle analysis of 124 years using observed rainfall datasets for Seoul, Korea.

In terms of comparison with past drought events, we noted that Seoul, Korea (WMO 47108) suffered from two high intensity events deduced by the projected periodic drought cycle of 124 years using data for over 240-years of rainfall records. The first event was a drought with peak intensity of −5.47 (27th April 1902) and the next with −3.46 (25th April 1778) in addition to the 28 years of successively weak and severe drought events prior and post these dates (Byun et al., 2008) (http://atmos.pknu.ac.kr/~intra3/). Therefore, it is obvious to believe that the next severe drought can occur in 2026. Interestingly this event coincides with the period EP in the present study using dynamic climate model data and differs only by 1 year between the predictions of Byun et al. (2008) using observed datasets. While the exact cause of this intense drought is unclear and presumably beyond the scope of our study, the 124 years periodicity of drought in earlier studies (Duhau and De Jager, 2010) has postulated to be linked with sunspot activities. Although global warming can potentially result in milder drought despite an increase in precipitation in some regions, future drought events are projected to be stronger, and therefore, a direct threat to water resource sectors, ecosystems, agriculture and humanity.

2.5. Regional analysis of future drought

2.5.1. Regional clustering

To examine regional changes in drought, a cluster analysis was conducted by using the Statistical Package for the Social Sciences (SPSS). The within-group linkage and the hierarchical clustering analysis method in SPSS were performed using the lowest value of the monthly *EDI* extracted from 678 grids in Korea for the period 2014–2100. This clustering technique groups clusters in order of similarity that was measured by the Pearson correlation coefficient. The number of optimum cluster was determined when the similarity between merged clusters decreased sharply (clusters between 4 and 3 in Fig. 6a) according to the number of groups. For a much greater depth of information, the readers are referred to Kim et al. (2011). Subsequently, the grids with similar trends in the lowest monthly *EDI* were grouped into four different clusters. Fig. 6b shows their spatial distribution where the region G1 corresponds to Northwest, G2 the Middle, G3 the Northeast and G4 the Southern region.

2.5.2. Seasonal changes in drought projections

Fig. 7 displays the percentage of the number of drought days (per month) for all three future periods. A prominent observation

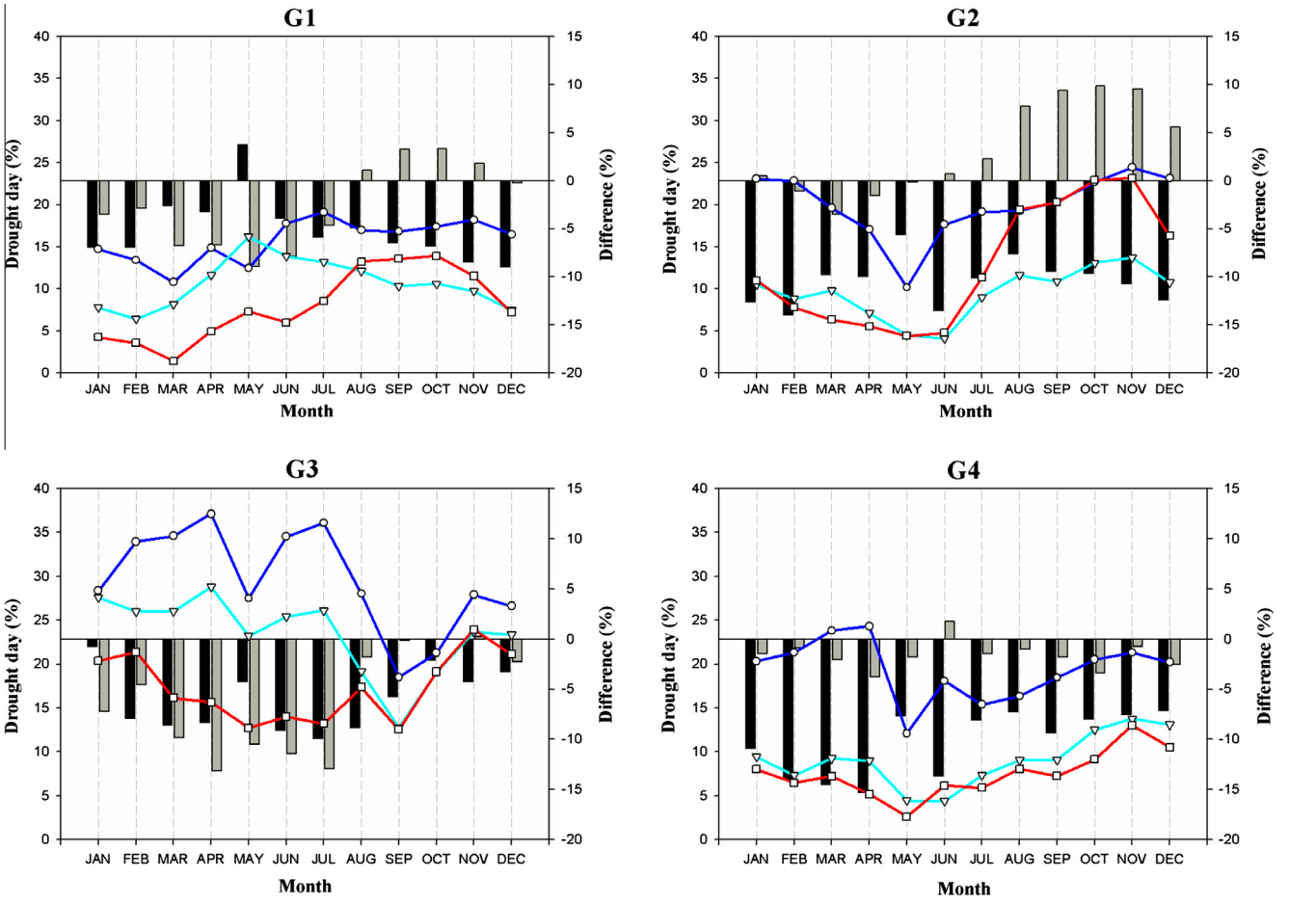

Fig. 7. Monthly percentage of drought days for the early (EP, circle with blue line), the middle (MP, triangle with cyan line), and the latter phase (LP, rectangle with red line) for each cluster. Black and grey bar are the differences between the middle and the early phase, the latter and the middle phase, respectively. (For interpretation of the references to color in this figure legend, the reader is referred to the web version of this article.)

is the significantly large percentage of drought days for the period EP relative to the other periods for all regions. This, however, appears to be especially pronounced in G3. These results coincide with our previous findings in Fig. 4, Tables 2 and 3 and also that of Byun et al. (2008), which predicted a severe drought event in the year 2025 based on a drought periodicity of 124 years. The next observation is the rapid increase in the number of drought days for the LP curve from August to November in G2 where the effect of ocean is supposed to be the smallest of four regions. This trend is seen also at G1 and coincides with the general results that global warming effect is not significant during the warm ocean season in these regions.

2.5.3. Annual changes and drought occurrence cycles

To examine annual intensity of drought in each sub-region, the minimum *EDI* per year for each grid cluster has been averaged (Fig. 8). The possibility of strong drought events (with low magnitudes of *EDI*) is exhibited from mid-2020s to the mid-2040s for the time-slice corresponding to *EP*. Again, the projected incidences in annual drought severity concur with the findings in Fig. 4, Tables 2 and 3 and Fig. 7 as well the previous observations of Byun et al. (2008).

It is noteworthy that extremely severe annual drought cases with *EDI* thresholds less than −2.0 basically appear in 3 groups. That is to say, considered by the region the year 2033 (for G3 and G4) and 2034 (for G2 and G3) shows peak of annual intensity where these two regions are expected to experience intense events almost at the same time, in addition to the year 2027 (for G3) and 2041 (for G4). Moreover, the projections of G3 and G4 have the 1st and the 2nd most severe cases of drought relative to the entire period of investigation. This contradicts the findings in Table 2 when droughts are analysed by their region. Based on annual droughts by region, the most severe case is expected to occur not in 2041 but in 2027 where the lowest minimum *EDI* (−2.85) is detected. Interestingly, this prediction differs by only 2 years from the predicted year of 2025 for the future peak drought analysed by Byun et al. (2008). It is also found that the annual intensity of drought is expected to decrease gradually in general and this is particularly conspicuous for the region G4 where an increase in precipitation has been simulated (Fig. 2). Interestingly a statistically significant rise in annual drought cases is expected in the region G4 as verified by largest regression slope (0.0046) over 99% confidence level.

To examine the cyclic nature of drought, a wavelet spectrum analysis is performed. However, a general spectrum analysis of the occurrence cycle of drought using the entire *EDI* dataset may contain unnecessary information because it also considers the periodicity of flood as well as drought (Byun et al., 2008). To avoid this error, only the monthly lowest *EDI* were used. Fig. 9 disseminates the results of each sub-region from the year 2014 to 2100. Evidently, G1 shows a strong periodicity in drought from the 2040s to 2070s. This periodicity displays repetitive cycles of 5 years at first and then changes to about 3.9 years in the early 2050s. G2 does not exhibit a significant drought cycle despite a strong periodicity of about 6 years around the 2050s. G3 showed a strong periodicity from the 2020s to the 2030s and 2060s. This

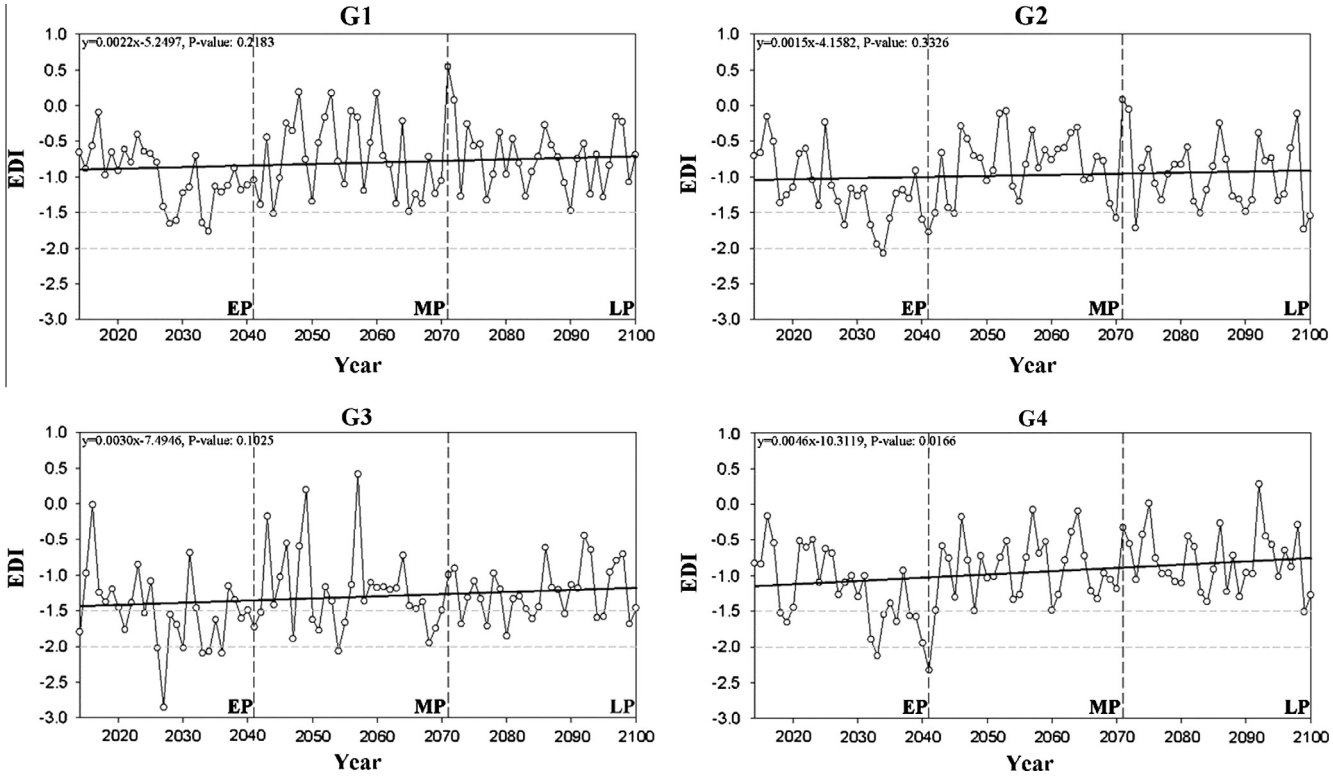

Fig. 8. Annual intensity of drought for each group. The thick solid line shows linear regression.

periodicity is based on a cycle of 6.6 years. Relatively short strong periodicity also appears in the 2020s and 2050s, but there is no significant cycle within the acceptable confidence levels except for the cycle of 6.6 years. In G4, as with the case of G2, a strong periodicity appears in the middle, but no significant cycle has been found.

To verify drought cycles detected in wavelet analysis, comparisons with years of severe to extreme drought with measured with *EDI* thresholds less than −1.5 are conducted (Fig. 8). In case of G3, the severe drought year emerges with a periodicity of almost 5–7 years from the 2020s to the 2050s and from 2080s to the 2090s. This is in agreement with wavelet spectrum analysis.

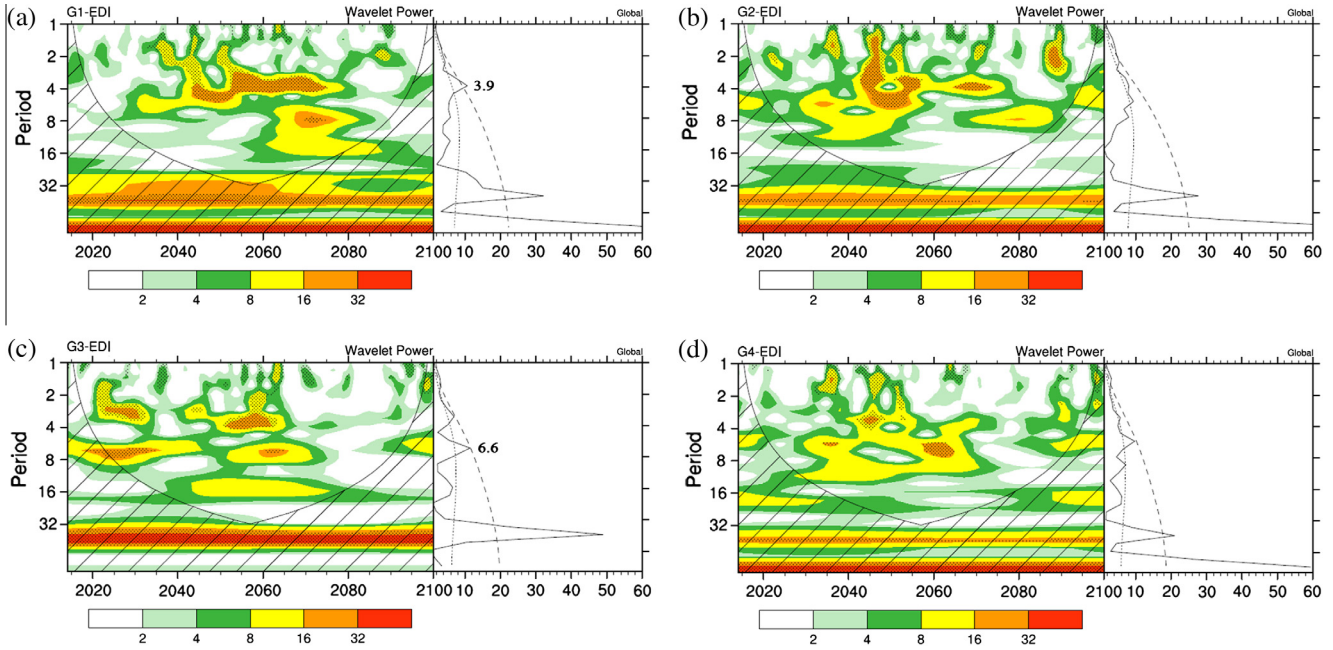

Fig. 9. Wavelet power spectrum (Morlet wavelet) conducted on the *EDI* series. (a) G1, (b) G2, (c) G3, and (d) G4 from 2014 to 2100. Black dotted area indicates 90% confidence level, using a red-noise background spectrum. The hatched area is the "cone of influence," in which edge effects are important. The panels on the right in (a)–(d) show the global power spectrum, i.e., the average of the wavelet power spectrum over time. The dotted and dashed lines show 50% and 90% confidence levels against red noise, respectively. (For interpretation of the references to color in this figure legend, the reader is referred to the web version of this article.)

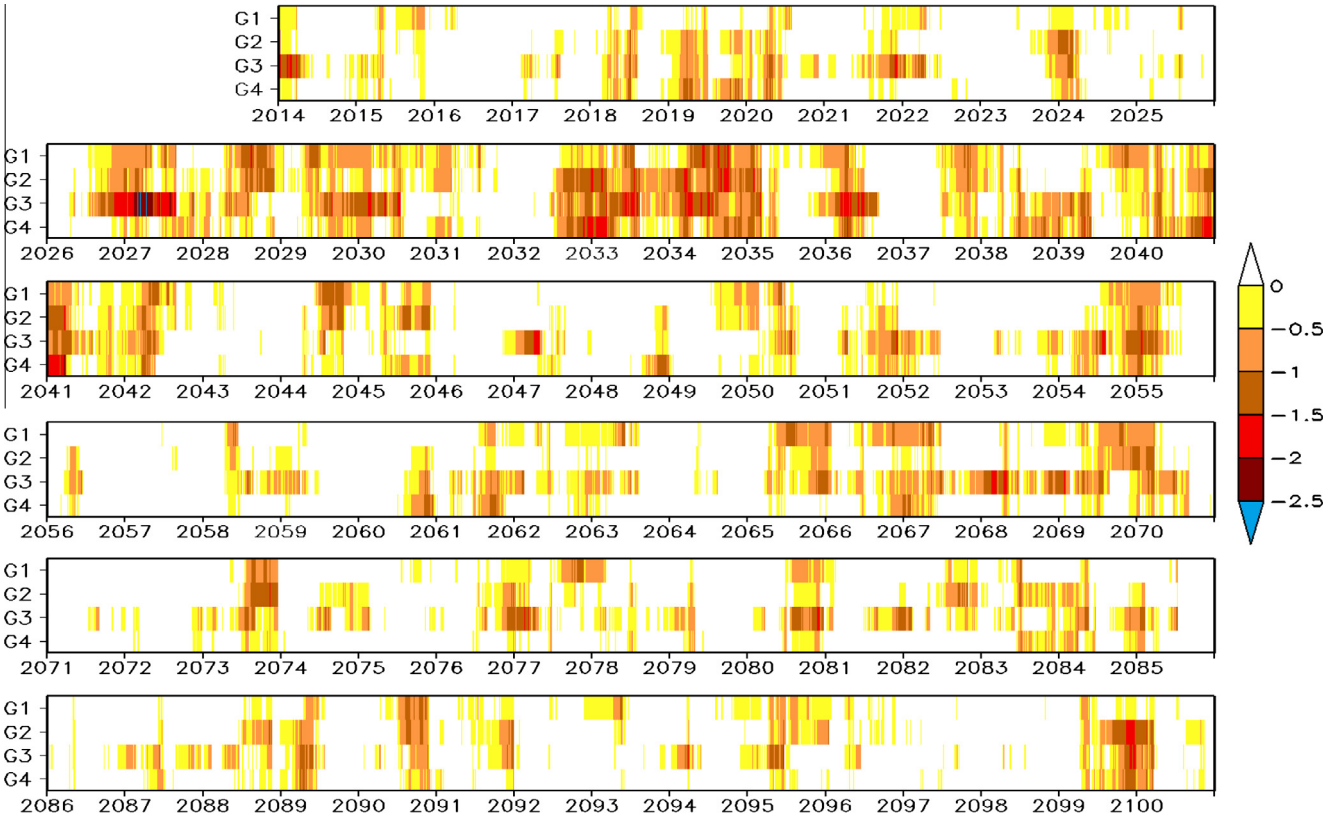

Fig. 10. Spatial–temporal drought map from 2014 to 2100. G1, G2, G3, and G4 denote the regions.

Indeed, this sort of drought cycle has been also revealed in past studies on drought periodicity (e.g. Min et al., 2003; Byun et al., 2008). Moreover, in the region G1, unlike the case of G3, the severe drought year does not appear with the cycle of 3.9 years in Fig. 8.

2.5.4. Spatial–temporal drought mapping

A spatial–temporal drought map is created to demonstrate regional and temporal distribution of future drought (Fig. 10). The map shows that future droughts are projected to frequently occur in all regions, especially from the mid-2020s to the early 2040s. These can be long lasting and intense and in general, agree with the highest frequency, intensity and duration in the EP found in previous analysis (Fig. 4). The droughts in G3 between the year 2026 and 2027 are distinct from the other regions in the same period. These were previously confirmed to be quite intense over annual timescales (Fig. 8). For the period 2032–2035, intense droughts are expected to occur nationwide, which may also continue in regions G2 and G3 but weaken temporarily in the middle of region G1 and G4. After this period, sporadic drought is expected to occur in some regions, with more intense ones from the mid-2060s in the region G1 and G3. Lastly, in the year 2099, a short, intensive drought is expected to occur in all regions, except G1.

3. Summary

The occurrence of future drought in Korea was predicted based on daily precipitation projections using the regional climate model, HadGEM3-RA and RCP 8.5 warming scenario for the period 2014–2100. The Effective Drought Index (*EDI*) initially developed by Byun and Wilhite (1999), was employed for identifying the onset of future drought as the date on which the *EDI* first dropped below −0.5 and secession when the *EDI* last exceeded this value while being consecutively negative after the onset in case of the minimum *EDI* less than −1.0. Therefore, the onset dates, duration, severity and intensity of future drought were deduced.

In order to analyse future drought, the precipitation projections were partitioned into the early (2014–2040), middle (2041–2070) and latter (2071–2100) phases while the study area was divided into 4 clusters (G1≡ Northwest, G2≡ Middle, G3≡ Northeast, and G4≡ Southern). It was revealed that the properties of future drought events could be diagnosed more precisely and quantitatively using the *EDI* without subjective assumptions other than those in Eq. (1). Accordingly, the characteristics of drought events were detected as follows:

1. The most severe drought was predicted to occur in the year 2027 for the region G3. This prediction was almost in parity with the year 2025 deduced previously by Byun et al. (2008) using historically observed data with a periodicity of 124-years.
2. The coastal areas in Korea exhibited continuous increase in future precipitation. However, the drought events were shown to become milder, especially in the southern coast as a consequence of global warming. This result stood at odds with some of the previous studies, and therefore requires more in-depth investigation. In other areas, however, the largest future precipitation appeared to be concentrated in the middle period, which had little correlation with global warming.
3. Based on wavelet and spectrum analysis, a periodicity in drought of about 6.6 years was deduced for the region G3. This finding concurred with the drought interval of 6 years previously found by Min et al. (2003) and Byun et al. (2008) using historically observed datasets.

4. Using regional clusters and the time-series of drought properties, a map of future drought occurrence over Korea was constructed. This offered a distinct advantage for identifying the drought intensity and duration by the year and the region simultaneously. This provided an easy and precise identification of future drought properties.

A significant outcome was the quantitative predictability of drought in Korea using the Effective Drought Index within the framework of a regional climate model (HadGEM3-RA) and RCP 8.5 warming scenario. The information on future drought disseminated generally reliable results compared with previous studies that used observed datasets. Conclusively, the prediction of future drought in Korea provides emphatic reference data for setting further research and drought response policies in the Korean region.

Acknowledgments

This work was supported by a Research Grant of Pukyong National University (2013 Year) Republic of Korea. We thank all reviewers and the Editorial Board of the Special Issue for their constructive comments on initial draft of the paper.

References

Boo, K.O., Kwon, W.T., Oh, J.H., Baek, H.J., 2004. Response of global warming on regional climate change over Korea: an experiment with the MM5 model. Geophys. Res. Lett. 31 (21).

Burke, E.J., 2011. Understanding the sensitivity of different drought metrics to the drivers of drought under increased atmospheric CO_2. J. Hydrometeorol. 12 (6), 1378–1394.

Burke, E.J., Brown, S.J., 2008. Evaluating uncertainties in the projection of future drought. J. Hydrometeorol. 9 (2), 292–299.

Burke, E.J., Brown, S.J., Christidis, N., 2006. Modeling the recent evolution of global drought and projections for the twenty-first century with the Hadley Centre climate model. J. Hydrometeorol. 7 (5), 1113–1125.

Byun, H.R., Han, Y.H., 1994. On the existence of the seasonal drought in the Korean Peninsula. Asia-Pac. J. Atmos. Sci. 30, 457–467.

Byun, H.R., Wilhite, D.A., 1999. Objective quantification of drought severity and duration. J. Clim. 12 (9), 2747–2756.

Byun, H.R., Lee, S.J., Morid, S., Choi, K.S., Lee, S.M., Kim, D.W., 2008. Study on the periodicities of droughts in Korea. Asia-Pac. J. Atmos. Sci. 44 (4), 417–441.

Chen, H., Sun, J., Chen, X., 2013. Future changes of drought and flood events in China under a global warming scenario. Atmos. Ocean. Sci. Lett..

Dai, A., 2013. Increasing drought under global warming in observations and models. Nat. Clim. Change 3 (1), 52–58.

Dogan, S., Berktay, A., Singh, V.P., 2012. Comparison of multi-monthly rainfall-based drought severity indices, with application to semi-arid Konya closed basin, Turkey. J. Hydrol. 470, 255–268.

Duhau, S., De Jager, C., 2010. The forthcoming grand minimum of solar activity. J. Cosmol. 8, 1983–1999.

Golmohammadi, M., Kamal, A., Bovani, A.M., 2011. The investigation of drought values fluctuation under the effect of climate change—case study: Gharesou Basin, Reston, VA: ASCE [at]. In: Proceedings of the 2011 World Environmental and Water Resources Congress, May 22–26, 2011, Palm Springs, California| d 20110000, American Society of Civil Engineers.

Hewitt, H. et al., 2011. Design and implementation of the infrastructure of HadGEM3: the next-generation Met Office climate modelling system. Geosci. Model Dev. 4 (2), 223–253.

Jones, P. et al., 1996. Summer moisture availability over Europe in the Hadley Centre general circulation model based on the Palmer Drought Severity Index. Int. J. Climatol. 16 (2), 155–172.

Karl, T.R., 1986. The sensitivity of the Palmer drought severity index and Palmer's *Z*-index to their calibration coefficients including potential evapotranspiration. J. Climate Appl. Meteorol. 25 (1), 77–86.

Ke, L., Da-Bang, J., Jian-Yong, M., 2012. Drought over China in the 21st century: results of RegCM3. Atmos. Ocean. Sci. Lett. 5 (6), 509–513.

Kim, D.W., Byun, H.R., 2009. Future pattern of Asian drought under global warming scenario. Theoret. Appl. Climatol. 98 (1–2), 137–150.

Kim, D.W., Byun, H.R., Choi, K.S., 2009. Evaluation, modification, and application of the Effective Drought Index to 200-year drought climatology of Seoul, Korea. J. Hydrol. 378 (1), 1–12.

Kim, D.W., Choi, K.S., Lee, J., Byun, H.R., 2010. Impact of climate change on the East Asia droughts. Advances in Geosciences. Atmos. Sci. (AS) 16, 165.

Kim, C.J., Park, M.J., Lee, J.H., 2014. Analysis of climate change impacts on the spatial and frequency patterns of drought using a potential drought hazard mapping approach. Int. J. Climatol. 34 (1), 61–80.

Kwak, J.W., Kyoung, M.S., Kim, D.G., Kim, H.S., 2011. Impact of climate change on SPI and SAD curve. World Environ. Water Res. Congr..

Lee, J.H., Kim, C.J., 2013. A multimodel assessment of the climate change effect on the drought severity–duration–frequency relationship. Hydrol. Process. 27 (19), 2800–2813.

Loukas, A., Vasiliades, L., Tzabiras, J., 2008. Climate change effects on drought severity. Adv. Geosci. 17 (17), 23–29.

Manabe, S., Wetherald, R.T., Milly, P., Delworth, T.L., Stouffer, R.J., 2004. Century-scale change in water availability: CO_2-quadrupling experiment. Clim. Change 64 (1–2), 59–76.

McKee, T.B., Doesken, N.J., Kleist, J., 1993. The relationship of drought frequency and duration to time scales. Proceedings of the 8th Conference on Applied Climatology. American Meteorological Society, Boston MA, pp. 179–183.

Mitchell, J., Warrilow, D., 1987. Summer dryness in northern mid-latitudes due to increased CO_2. Nature 330 (6145), 238–240.

Morid, S., Smakhtin, V., Moghaddasi, M., 2006. Comparison of seven meteorological indices for drought monitoring in Iran. Int. J. Climatol. 26 (7), 971–985.

Moss, R.H. et al., 2010. The next generation of scenarios for climate change research and assessment. Nature 463 (7282), 747–756.

Nakićenović, N.a., 2000. Summary for policymakers: emission scenarios: a special report of Working Group III of the intergovernmental panel on climate change. Intergovern. Panel Clim. Change.

Palmer, W.C., 1965. Meteorological drought. US Department of Commerce, Weather Bureau, Washington, DC, USA.

Palutikof, J., Winkler, J., Goodess, C., Andresen, J., 1997. The simulation of daily temperature time series from GCM output. Part I: Comparison of model data with observations. J. Clim. 10 (10), 2497–2513.

Portman, D.A., Wang, W.-C., Karl, T.R., 1992. Comparison of general circulation model and observed regional climates: daily and seasonal variability. J. Clim. 5 (4), 343–353.

Rhee, J., Carbone, G.J., 2007. A comparison of weekly monitoring methods of the Palmer Drought Index. J. Clim. 20 (24), 6033–6044.

Riahi, K. et al., 2011. RCP 8.5—a scenario of comparatively high greenhouse gas emissions. Clim. Change 109 (1–2), 33–57.

Rind, D., Goldberg, R., Hansen, J., Rosenzweig, C., Ruedy, R., 1990. Potential evapotranspiration and the likelihood of future drought. J. Geophys. Res.: Atmos. (1984–2012) 95 (D7), 9983–10004.

Sheffield, J., Wood, E.F., 2008. Projected changes in drought occurrence under future global warming from multi-model, multi-scenario, IPCC AR4 simulations. Clim. Dyn. 31 (1), 79–105.

Skelly, W.C., Henderson-Sellers, A., 1996. Grid box or grid point: what type of data do GCMs deliver to climate impacts researchers? Int. J. Climatol. 16 (10), 1079–1086.

Smith, D., Hutchinson, M., McArthur, R., 1993. Australian climatic and agricultural drought: payments and policy. Drought Network News 5 (3), 11–12.

Taylor, I. et al., 2012. Contributions to uncertainty in projections of future drought under climate change scenarios. Hydrol. Earth Syst. Sci. Discuss. 9 (11), 12613–12653.

Todd, B., Macdonald, N., Chiverrell, R., Caminade, C., Hooke, J., 2013. Severity, duration and frequency of drought in SE England from 1697 to 2011. Clim. Change 121 (4), 673–687.

Trenberth, K.E. et al., 2014. Global warming and changes in drought. Nat. Clim. Change 4 (1), 17–22.

Van Vuuren, D.P. et al., 2011. The representative concentration pathways: an overview. Clim. Change 109, 5–31.

Vidal, J.P., Wade, S., 2009. A multimodel assessment of future climatological droughts in the United Kingdom. Int. J. Climatol. 29 (14), 2056–2071.

Vidal, J.-P., Martin, E., Kitova, N., Najac, J., Soubeyroux, J.-M., 2012. Evolution of spatio–temporal drought characteristics: validation, projections and effect of adaptation scenarios. Hydrol. Earth Syst. Sci. 16 (8), 2935–2955.

Wang, G., 2005. Agricultural drought in a future climate: results from 15 global climate models participating in the IPCC 4th assessment. Clim. Dyn. 25 (7–8), 739–753.

Wetherald, R.T., Manabe, S., 2002. Simulation of hydrologic changes associated with global warming. J. Geophys. Res.: Atmos. (1984–2012) 107 (D19). ACL 7-1–ACL 7-15.